International Journal of Heat and Mass Transfer 52 (2009) 1036–1043

Contents lists available at ScienceDirect

International Journal of Heat and Mass Transfer

journal homepage: www.elsevier.com/locate/ijhmt

Laminar natural convection in a square cavity: Low Prandtl numbers and large density differences

T. Pesso, S. Piva *

ENDIF, University of Ferrara, via Saragat n.1, Ferrara 44100, Italy

ARTICLE INFO

Article history:
Received 3 January 2007
Available online 11 September 2008

Keywords:
Natural convection
Heat transfer correlation
Square cavity
Variable properties

ABSTRACT

Steady natural convection at low Prandtl numbers caused by large density differences in a square cavity heated through the side walls is investigated numerically and theoretically. An appropriate dimensionless parameter characterizing the density differences of the working fluid is identified by the Gay-Lussac number. The Boussinesq assumption is achieved when the Gay-Lussac number tends to zero. The Nusselt number is derived for the ranges in Rayleigh number $10 \leqslant Ra \leqslant 10^8$, in Prandtl number $0.0071 \leqslant Pr \leqslant 7.1$ and in Gay-Lussac number $0 \leqslant Ga < 2$. The effects of the Rayleigh, Prandtl and Gay-Lussac numbers on the Nusselt number are discussed on physical grounds by means of a scale analysis. Finally, based on physical arguments, a heat transfer correlation is proposed, valid for all Prandtl and Gay-Lussac number ranges addressed.

1. Introduction

Natural convection in cavities has been intensively studied in the literature due to its relevance to many fields of science and technology such as geophysics, nuclear reactor systems, energy storage and foundry processes.

There are numerous studies in the literature regarding natural convection in cavities, a considerable amount of which is reviewed by Ostrach [1]. In particular, rectangular and square cavities are the most frequently studied due to their many thermo-fluid features, such as recirculation and stagnation regions, boundary layers, jet deflection, and thermal entrainment.

In the case of natural convection in cavities due only to temperature differences, in absence of both heat generation and concentration gradients, three main configurations have been considered in the literature:

(1) natural convection in horizontal layers heated through the top and bottom walls;
(2) sideways heating of an initially stratified fluid layer;
(3) natural convection in enclosures heated through the side walls.

The square cavity has been regarded in the literature as the most suitable case for the validation of numerical codes for thermal analysis and for physical understanding of natural convection in enclosures.

De Vahl Davis [2] provided a well known set of benchmark solutions for steady natural convection of air in a horizontally heated square cavity for Rayleigh numbers up to 10^6. Le Quéré [3] extended the analysis up to $Ra = 10^8$.

The account of possible interactions between the fluid in an enclosure and its surroundings can also be of practical interest. The influence of participating walls has been analysed for instance by Costa [4], while the effect of solids located at the corners of the cavity has been investigated by Costa et al. [5]. However, in most of the papers [1] conductive walls are not included.

The working fluids analysed in the literature have been mainly air and water. In addition, due to the interest in foundry processes, crystal-growing and nuclear reactor systems, liquid metals have also been studied.

Braunsfurth et al. [6] presented numerical and experimental temperature profiles corresponding to laminar natural convection of liquid gallium in a rectangular cavity heated through the side walls. For the same problem, a simplified model was proposed by Graebel [7]: the heat transfer results have been derived analytically for the Prandtl number range from about 0.05 up to infinity. Lage and Bejan [8] studied laminar natural convection in a square enclosure heated through the side walls for $0.01 \leqslant Pr \leqslant 10$ and $10^2 \leqslant Ra \leqslant 10^{11}$ and addressed the influence of the Prandtl number on the heat transfer. A similar problem has been analysed for $0.011 \leqslant Pr \leqslant 0.054$ by Saravanan and Kandaswamy [9]: they observed a significant effect of a variable thermal conductivity on the heat transfer through the cavity. For liquid gallium, significant differences were also evident in a comparison between 2-D and 3-D numerical predictions carried out by Derebail and Koster [10].

* Corresponding author. Tel.: +39 0532 974816; fax: +39 0532 974870.
E-mail address: pvs@unife.it (S. Piva).

0017-9310/$ - see front matter © 2008 Elsevier Ltd. All rights reserved.
doi:10.1016/j.ijheatmasstransfer.2008.07.005

Nomenclature

c_p	specific heat at constant pressure
F'_B	buoyancy forces per unit depth
F'_I	inertial forces per unit depth
F'_v	viscous forces per unit depth
g	acceleration of gravity
Ga	Gay-Lussac number, $Ga = \beta_o \Theta$
h'	specific enthalpy
L	width of the cavity
$\mathbf{n}$	outward unit normal vector
Nu	average Nusselt number, Eq. (24)
Nu_y	local Nusselt number, Eq. (23)
$Nu_{y,max}$	maximum value of local Nusselt number
$Nu_{y,min}$	minimum value of local Nusselt number
p'	pressure
p	dimensionless pressure, $p = (p' + \rho_o g y')/P$
P	reference pressure, $P = \rho_o U^2$
Pr	Prandtl number, $Pr = \upsilon_o/\alpha_o$
Q'	heat flux per unit depth through an isothermal side of the cavity
q''	specific heat flux per unit depth
Ra	Rayleigh number, $Ra = g\beta_o \Theta L^3/(\alpha_o \upsilon_o)$
T'	temperature
T'_o	reference temperature, $T'_o = (T'_h + T'_c)/2$
T	dimensionless temperature, $T = (T'_o - T')/\Theta$
u', v'	Cartesian velocity components
u, v	dimensionless Cartesian velocity components, $u = u'/U$ and $v = v'/U$
U	reference velocity, $U = (g\beta_o L\Theta)^{1/2}$
V	characteristic vertical velocity on the thermal layer
x', y'	Cartesian co-ordinates
x, y	Cartesian dimensionless co-ordinates, x'/L and y'/L

Greek symbols

α	thermal diffusivity
β	volumetric coefficient of thermal expansion
δ_T	thermal layer thickness
λ	thermal conductivity
μ	dynamic viscosity
υ	kinematic viscosity
Θ	characteristic temperature difference, $\Theta = T'_h - T'_c$
ρ	density
Π_N	dimensionless parameter, Eq. (42)

Subscripts

c	cold wall
h	hot wall
o	at the reference temperature T'_o
r	at the reference temperature T'_r
w	wall
adv	advection
cond	conduction

In connection with advanced engineering applications in nuclear reactor systems, recent studies on natural convection in enclosures at low Prandtl numbers address the effects of magneto-hydrodynamic interactions and volumetric heating. Some representative studies can be found in [11–15].

The whole quoted papers [1–15] deal with the Boussinesq approximation. However, in many practical applications, the natural convection is driven by high temperature differences and, for these cases, the Boussinesq approach may be too restrictive because of the strong variations in the thermophysical properties of the working fluid. This is the case for instance of foundry processes. For these applications the study of natural convection in enclosures due to large temperature differences could provide important considerations in the design, both for more efficient operations and for higher quality manufactures.

In the literature, only a few studies have been undertaken to examine the influence of the variability of thermophysical properties on laminar natural convection in cavities.

In the case of heating through the side walls, variable physical properties have been considered by Zhong et al. [16]. They observed significant variable properties effects on the heat transfer and also suggested a limit of validity of the Boussinesq approximation and a heat transfer correlation.

Becker and Braack [17] provided numerical predictions for the case of laminar natural convection of a weakly compressible ideal gas (air) in a square cavity heated through the side walls. The same problem, but for a fully compressible ideal gas, has been analysed by Vierendeels et al. [18] and by Darabandi and Hosseinizadeh [19]. A very good agreement can be observed among the predictions in [17–19]. For the same problem, Paillere et al. [20] found a very good agreement between the results obtained by the weakly compressible and the fully compressible model. In these papers [17–20] the Mach number is always very low; for example, the highest local Mach number predicted in [20] was about of 10^{-4}.

It may be concluded from reviewing the literature that there is a lack of information on the influence of low and very low Prandtl numbers and of large density differences due to large temperature differences on heat transfer due to natural convection.

The present paper deals with these latter aspects. The analysis has been carried out for the case of laminar flow in a square cavity heated through the side walls.

The dimensionless parameter characterizing the density differences of the working fluid has been identified as the Gay-Lussac number. Its influence on the Nusselt number has been derived over its entire physical domain, where the limiting cases lead to the Boussinesq assumption and to extreme density variation, respectively.

Also, the influence of the Prandtl number on Nusselt number has been examined for $0.0071 \leqslant Pr \leqslant 7.1$. The Rayleigh number studied here ranges from 10 up to 10^8.

The governing equations were treated by the finite volume CFD commercial package ANSYS CFX-10.0 [21].

The numerical procedure has been validated by comparison against the results provided by de Vahl Davis [2], Le Quéré [3], Lage and Bejan [8] and Wan et al. [22].

The Nusselt number has been derived for the above ranges of *Ra*, *Pr* and *Ga* numbers.

Finally, a correlation relating the laminar Nusselt number to the above ranges of parameters has been proposed. Its development is based on physical arguments based on the conservation of momentum and thermal energy.

2. Mathematical formulation

The system to be considered (Fig. 1) is a two-dimensional square cavity of width L, where the two vertical walls are kept at different temperature, T'_h and T'_c. Zero heat flow is assumed at the top and bottom walls. The walls are rigid and impermeable, and no-slip boundary conditions are imposed at the boundaries.

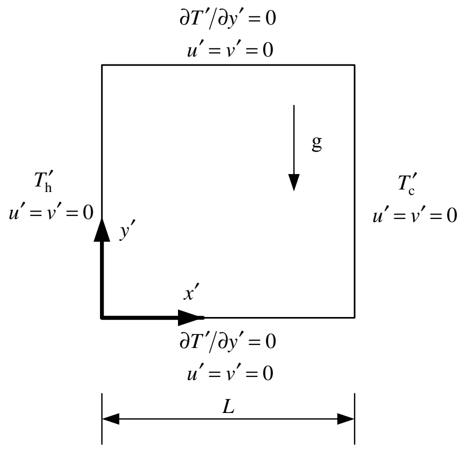

Fig. 1. Model of physical system and boundary conditions.

The flow is steady. The fluid is incompressible, Newtonian and its density is supposed to be linearly dependent on temperature in all the terms of the governing equations. The other thermophysical properties are considered constant at the reference temperature T'_o, which is posed equal to $(T'_h + T'_c)/2$. Viscous dissipation is neglected.

Based on the above assumptions, the following conservation equations were solved by the finite volume CFD commercial package ANSYS CFX-10.0 [21]:

Mass:

$$\frac{\partial}{\partial x'}(\rho u') + \frac{\partial}{\partial y'}(\rho v') = 0 \quad (1)$$

Momentum:

$$\frac{\partial}{\partial x'}(\rho u'u') + \frac{\partial}{\partial y'}(\rho v'u') = -\frac{\partial p'}{\partial x'} + \mu_o\left(\frac{\partial^2 u'}{\partial x'^2} + \frac{\partial^2 u'}{\partial y'^2} + \frac{1}{3}\left(\frac{\partial^2 u'}{\partial x'^2} + \frac{\partial^2 v'}{\partial x'\partial y'}\right)\right) \quad (2)$$

$$\frac{\partial}{\partial x'}(\rho u'v') + \frac{\partial}{\partial y'}(\rho v'v') = -\frac{\partial p'}{\partial y'} - \rho g + \mu_o\left(\frac{\partial^2 v'}{\partial x'^2} + \frac{\partial^2 v'}{\partial y'^2} + \frac{1}{3}\left(\frac{\partial^2 u'}{\partial x'\partial y'} + \frac{\partial^2 v'}{\partial y'^2}\right)\right) \quad (3)$$

Energy:

$$\frac{\partial}{\partial x'}(\rho u'h') + \frac{\partial}{\partial y'}(\rho v'h') = \lambda_o\left(\frac{\partial^2 T'}{\partial x'^2} + \frac{\partial^2 T'}{\partial y'^2}\right) \quad (4)$$

For the property assumptions above, the equation of state is given by:

$$\rho = \rho_o(1 + \beta_o(T'_o - T')) \quad (5)$$

When using Eq. (4) for liquid or gases with constant specific heat, the code ANSYS CFX-10.0 automatically neglects the dependency of the enthalpy on the pressure [21]. Then the specific enthalpy is given by:

$$h' = c_{p_o}(T' - T'_{ref}) + h'_{ref} \quad (6)$$

where the reference state is $h'_{ref} = 0$ J/kg at $T' = T'_{ref}$.

The boundary conditions are given by:

$$\left.\frac{\partial T'}{\partial y'}\right|_{y'=0,L} = 0 \quad (7)$$

$$T'(x' = 0) = T'_h \quad (8)$$

$$T'(x' = L) = T'_c \quad (9)$$

$$u'|_w = v'|_w = 0 \quad (10)$$

Eqs. (1)–(10) have been expressed in dimensionless form, according to the following dimensionless variables:

$$T = \frac{T'_o - T'}{\Theta}, \quad u = \frac{u'}{U}, \quad v = \frac{v'}{U}, \quad p = \frac{p' + \rho_o g y'}{P}, \quad x = \frac{x'}{L}, \quad y = \frac{y'}{L}$$

The characteristic quantities for this problem are:

$$\Theta = T'_h - T'_c, \quad U = \sqrt{g\beta_o L\Theta}, \quad P = \rho_o U^2$$

In particular, in the case of buoyancy-driven flows, the choice of the reference velocity U is not unique in the literature. A meaningful velocity scale must be related to the intensity of motion. For this reason, scales related to the molecular diffusivity as υ_o/L or α_o/L are unrealistic [23]. The choice $U = (g\beta_o L\Theta)^{1/2}$ may be thought of as a balance of the order of magnitude of the buoyancy forces and the inertial ones on the global length L and it is suitable when $(Ra/Pr)^{1/2} \gg 1$ [24].

The dimensionless conservation equations are given by:

Mass:

$$\frac{\partial}{\partial x}((1 + GaT)u) + \frac{\partial}{\partial y}((1 + GaT)v) = 0 \quad (11)$$

Momentum:

$$\frac{\partial}{\partial x}((1 + GaT)uu) + \frac{\partial}{\partial y}((1 + GaT)vu) = -\frac{\partial p}{\partial x} + \left(\frac{Pr}{Ra}\right)^{1/2}\left(\frac{\partial^2 u}{\partial x^2} + \frac{\partial^2 u}{\partial y^2} + \frac{1}{3}\left(\frac{\partial^2 u}{\partial x^2} + \frac{\partial^2 v}{\partial x\partial y}\right)\right) \quad (12)$$

$$\frac{\partial}{\partial x}((1 + GaT)uv) + \frac{\partial}{\partial y}((1 + GaT)vv) = -\frac{\partial p}{\partial y} - T + \left(\frac{Pr}{Ra}\right)^{1/2}\left(\frac{\partial^2 v}{\partial x^2} + \frac{\partial^2 v}{\partial y^2} + \frac{1}{3}\left(\frac{\partial^2 u}{\partial x\partial y} + \frac{\partial^2 v}{\partial y^2}\right)\right) \quad (13)$$

Energy:

$$\frac{\partial}{\partial x}((1 + GaT)uT) + \frac{\partial}{\partial y}((1 + GaT)vT) = (Pr\,Ra)^{-1/2}\left(\frac{\partial^2 T}{\partial x^2} + \frac{\partial^2 T}{\partial y^2}\right) \quad (14)$$

The boundary conditions are expressed in non-dimensional form as follows:

$$\left.\frac{\partial T}{\partial y}\right|_{y=0,1} = 0 \quad (15)$$

$$T(x = 0) = T_h = -1/2 \quad (16)$$

$$T(x = 1) = T_c = 1/2 \quad (17)$$

$$u|_w = v|_w = 0 \quad (18)$$

The dimensionless numbers are given by:

$$Pr = \frac{\upsilon_o}{\alpha_o}, \quad Ra = \frac{g\beta_o\Theta L^3}{\alpha_o\upsilon_o}, \quad Ga = \beta_o\Theta$$

It may be observed that the dimensionless problem, Eqs. (11)–(18), shows a dimensionless parameter, the Gay-Lussac number, not present in the case under the Boussinesq assumption. This parameter quantifies the density differences of the working fluid under the temperature field. From Eqs. (11)–(18) it may be seen that the Boussinesq assumption is achieved as Ga tends to zero with fixed Ra and Pr.

In the literature a Gay-Lussac number is quoted without any explanations, for instance, in the compilations due to Catchpole and Fulford [25] and Hahnemann [26], where is presented as $1/Ga$. The present Ga has been used to analyse the mixed convection in reactors [27–32]; the main difference with the present work stands in the fully compressible ideal gas model used in [27,28] and in the ideal gas in isobaric transformations used in [29–32].

Furthermore, in the case of natural convection in cavities with large temperature differences, a parameter with the same meaning of the present *Ga* has been also referred to *temperature difference ratio* [16], *relative temperature difference* [17], *temperature difference parameter* [19,33], *dimensionless temperature difference* [34,35], or simply *dimensionless parameter* [18,20]. This dimensionless parameter is equal to $Ga/(1 - Ga/2)$ in [16], $Ga/2$ in [17–20,34,35] and *Ga* in [33], respectively.

The specific and the overall heat flux per unit depth are given by:

$$q''_{h,c} = \lambda_o (\nabla T \cdot \boldsymbol{n})_{h,c} \tag{19}$$

$$Q'_{h,c} = \int_0^L q''_{h,c} \, dy' \tag{20}$$

The local and mean Nusselt numbers are given by:

$$Nu_y = \frac{q''_h L}{\lambda_o \Theta} \tag{21}$$

$$Nu = \frac{Q'_h}{\lambda_o \Theta} \tag{22}$$

According to the previously defined rules of adimensionalization and to Eqs. (19) and (20), Eqs. (21) and (22) become:

$$Nu_y = \left.\frac{\partial T}{\partial x}\right|_h \tag{23}$$

$$Nu = \int_0^1 \left.\frac{\partial T}{\partial x}\right|_h dy \tag{24}$$

The set of Eqs. (1)–(10) were solved by a finite volume technique using the CFD commercial package ANSYS CFX-10.0 [21].

A base non-equispaced grid 52×52 (first cell dimension = $2 \times 10^{-3}L$, expansion factor = 1.1602) was selected as a trade-off between numerical accuracy and computation time. However, for $10^6 \leqslant Ra \leqslant 10^8$ only the use of finer grids (102×102 grid, first cell dimension = $1 \times 10^{-3}L$, expansion factor = 1.0739; 204×204 grid, first cell dimension = $5 \times 10^{-4}L$, expansion factor = 1.0361) assured the same level of accuracy of the base grid.

Second Order Upwind Differencing Scheme (SOUDS) and Upwind Differencing Scheme (UDS) were used for $Pr > 0.01$ and $Pr \leqslant 0.01$, respectively. In particular, for the lowest Prandtl numbers addressed in the present paper, UDS provided the best performance, both in terms of accuracy and numerical convergence.

Different under relaxation factors were used depending on the value of the Prandtl number. For $Pr > 0.071$, a 0.9 under relaxation factor was used just for the momentum equations, Eqs. (2) and (3). For $Pr \leqslant 0.071$, 0.08 and 0.1 under relaxation factors were used for the momentum, Eqs. (2) and (3), and energy, Eq. (4), equations, respectively.

Finally, the following criterion to check for the steady-state solution was used:

$$\left| \frac{Q'_h + Q'_c}{Q'_h} \right| \leqslant 10^{-4} \tag{25}$$

3. Results and discussion

The numerical procedure has been validated by comparison against the results provided by Lage and Bejan [8], de Vahl Davis [2], Wan et al. [22] and Le Quéré [3]. These results have been derived under the Boussinesq assumption.

The comparison is summarized in Table 1. For $Pr = 0.01$ a very good agreement between the present predictions and those provided by Lage and Bejan [8] can be observed. For $Pr = 0.71$ and $Ra = 10^3$, 10^4 and 10^5 the present predictions are in a very good agreement with the data provided by de Vahl Davis [2] and in a fairly good agreement with those provided by Wan et al. [22]. For $Pr = 0.71$ and $Ra = 10^6$ a very good agreement with the predictions provided by Le Quéré [3] and those provided by de Vahl Davis [2] is evident; an appreciable difference is still evident with the predictions provided by Wan et al. [22]. For $Pr = 0.71$ and $Ra = 10^7$ and 10^8 a very fine grid (204×204) provided a very good agreement with Le Quéré [3], while the agreement with the results provided by Wan et al. [22] is still fairly good.

Table 1
Comparison of present predictions with previous works for different Prandtl numbers – Boussinesq

			Nu	$Nu_{y,max}$	$Nu_{y,min}$
Pr 0.01	Ra 10^4	Lage and Bejan [8]	1.50	–	–
		Present predictions 52×52	1.493	–	–
	Ra 10^5	Lage and Bejan [8]	2.77	–	–
		Present predictions 52×52	2.763	–	–
Pr 0.71	Ra 10^3	de Vahl Davis [2]	1.118	1.505	0.692
		Wan et al.[22]	1.117	1.501	0.691
		Present predictions 52×52	1.116	1.502	0.692
	Ra 10^4	de Vahl Davis [2]	2.243	3.528	0.586
		Wan et al.[22]	2.254	3.579	0.577
		Present predictions 52×52	2.242	3.533	0.584
	Ra 10^5	de Vahl Davis [2]	4.519	7.717	0.729
		Wan et al.[22]	4.598	7.945	0.698
		Present predictions 52×52	4.521	7.728	0.729
	Ra 10^6	de Vahl Davis [2]	8.800	17.925	0.989
		Wan et al.[22]	8.976	17.86	0.9132
		Le Quéré [3]	8.825	17.536	0.9795
		Present predictions 102×102	8.827	17.55	0.980
	Ra 10^7	Wan et al.[22]	16.656	38.6	1.298
		Le Quéré [3]	16.523	39.39	1.366
		Present predictions 102×102	16.55	39.61	1.367
	Ra 10^8	Wan et al.[22]	31.486	91.16	1.766
		Le Quéré [3]	30.225	87.24	1.919
		Present predictions 204×204	30.26	87.79	1.919

In order to investigate the influence of the Prandtl and Gay-Lussac numbers on the laminar mean Nusselt number, further computations have been carried out for different values of dimensionless parameters.

The Prandtl number range $0.0071 \leqslant Pr \leqslant 7.1$ has been considered. Following the suggestions by Lage and Bejan [8], in order to assure laminar flow solutions, this range was split in $0.0071 \leqslant Pr < 0.71$ and $0.71 \leqslant Pr \leqslant 7.1$, for $10 \leqslant Ra \leqslant 10^5$ and $10 \leqslant Ra \leqslant 10^8$, respectively.

The Gay-Lussac number range $0 \leqslant Ga < 2$ has been considered. The density must obviously be always positive. Taking into consideration that the lowest density is reached along the hot wall, from the dimensionless form of Eq. (5) it follows:

$$(1 + GaT_h) > 0 \tag{26}$$

and the upper bound for *Ga* (Eq. (16)) becomes:

$$Ga < 2 \tag{27}$$

Consequently, it was investigated only for the limit of the mean Nusselt number as *Ga* approaches 2, taking into account values only very close to 2, namely $Ga = 1.95–1.98$.

In Fig. 2 the influence of the Prandtl number on the mean Nusselt number for $Ga = 0.3$ and $10^3 \leqslant Ra \leqslant 10^5$ is shown. For a fixed Gay-Lussac number, *Nu* increases as *Pr* increases. In particular the effect of the Prandtl number is more evident as the Rayleigh number increases.

In Fig. 3 the influence of the Gay-Lussac number on the mean Nusselt number for $0.0071 \leqslant Pr \leqslant 7.1$ and $10^3 \leqslant Ra \leqslant 10^5$ is shown. The abscissa has been bounded by the value $Ga = 1.5$, since for values of *Ga* very close to 2 the results only have a mathematical meaning, not a physical one. In the range of analysis, for fixed val-

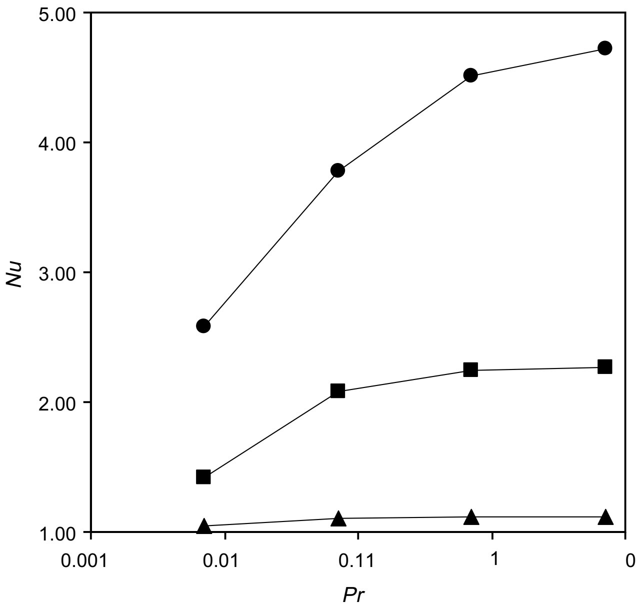

Fig. 2. Influence of the Prandtl number on the mean Nusselt number ($Ga = 0.3$) – ▲ Ra 10^3; ■ Ra 10^4; ● Ra 10^5.

ues of Ra and Pr, when the density varies in the whole terms of the conservation equations, the mean Nusselt number is always lower than that calculated under the Boussinesq model ($Ga = 0$, Ra and Pr fixed). The difference between $Nu(Ga > 0$, Ra and Pr fixed) and $Nu(Ga = 0$, Ra and Pr fixed) is not appreciable when $Ga < 0.3$. The highest differences are achieved when $Ga = 1.5$ and varies from about 1% to 7%, as the Rayleigh number increases from 10^3 to 10^5.

4. Scale analysis

A scale analysis has been developed in order to investigate in physical terms the influence on the mean Nusselt number of the dimensionless parameters as used here. Furthermore, on the basis of the present scale analysis, a single dimensionless quantity Π_N has been introduced to correlate the present Nu predictions.

Procedures already available in the literature have been the starting point for the present analysis. Bejan [36] used the vertical boundary layer approximation for the scale analysis for natural convective Boussinesq flows in enclosures: the analysis is performed in limiting situations, for very low and very high Prandtl numbers. This approach has been extended to the entire Prandtl number range by Arpaci [37] for microscale buoyant turbulent flows and by Arpaci and Agarwal [38] for turbulent ceiling fires. Aydin and Guessoues [39] developed further on the methodology in the case of free convection from an uniformly heated vertical plate.

Unlike [36–39], the present calculations show a thermal boundary layer adjacent to the heated and cooled walls only for $Ra \geqslant 10^5$. As a consequence, in the present analysis the boundary layer approach has been not used.

Referring to the heated side wall, for the present analysis the following scale parameters are used:

- Length scales: $x' \approx \delta_t$, $y' \approx L$.
- Velocity scales: $v' \approx V$, $u' \approx V \cdot \delta_t / L$.
- Temperature scales: $T' \approx \Theta$, $(T'_o - T') \approx -\Theta$.

where δ_t is the thickness of the thermal layer where the heat diffusion is assumed to be confined, V is the local vertical velocity scale on the thermal layer δ_t. The scale $u' \approx V \cdot \delta_t / L$ derives from mass

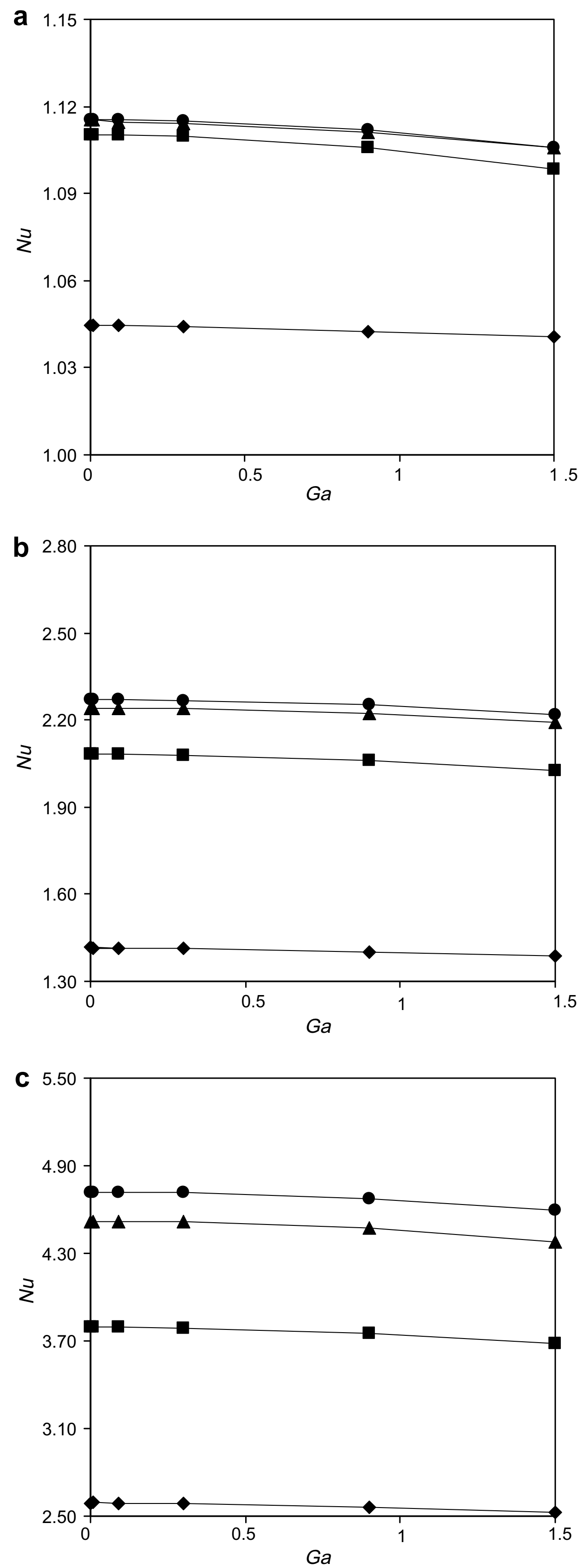

Fig. 3. Influence of the Gay-Lussac number on the mean Nusselt number – (a) Ra 10^3, (b) Ra 10^4, (c) Ra 10^5 – (♦ Pr 0.0071; ■ Pr 0.071; ▲ Pr 0.71; ● Pr 7.1).

conservation, while the temperature scale $(T'_o - T') \approx -\Theta$ has been considered since $T' \geqslant T'_o$ for $0 \leqslant x' \leqslant \delta_t$.

First of all, the mean Nusselt number, Eq. (22), has been related to the scales of the problem. The order of magnitude of the heat flux through the hot side of the cavity, Q'_h, Eq. (20), according to the scales of this problem, becomes:

$$Q'_h \approx \lambda_o \frac{\Theta}{\delta_t} L \quad (28)$$

Therefore, the order of magnitude of the mean Nusselt number, following Eq. (22), becomes:

$$Nu \approx L/\delta_t \quad (29)$$

In Eqs. (28) and (29) the only unknown is the thermal layer thickness δ_t. This quantity can be obtained considering both the integral energy and vertical momentum balances over the thermal layer.

The thermal energy balance over the thermal layer δ_t expresses a balance between the heat transported by advection, Q'_{adv}, and that transported by conduction, Q'_{cond}:

$$Q'_{adv} \approx Q'_{cond} \quad (30)$$

When replacing the flux through a closed surface with the corresponding volume integral, these two quantities, Eq. (30), may be expressed as follows:

$$Q'_{adv} = \int_0^L \int_0^{\delta_t} c_{p_o} \rho_o (1 + \beta_o (T'_o - T')) \left(u' \frac{\partial T'}{\partial x'} + v' \frac{\partial T'}{\partial y'} \right) dx' \, dy' \quad (31)$$

and:

$$Q'_{cond} = \int_0^L \int_0^{\delta_t} \lambda_o \left(\frac{\partial^2 T'}{\partial x'^2} + \frac{\partial^2 T'}{\partial y'^2} \right) dx' \, dy' \quad (32)$$

According to Eqs. (31) and (32) and the scales of the problem, the energy balance, Eq. (30), becomes:

$$\left[\rho_o c_{p_o} (1 - (\approx Ga)) V \frac{\Theta}{L} \delta_t L \right] \approx \left[\lambda_o \frac{\Theta}{\delta_t^2} \left(1 + \approx \frac{\delta_t^2}{L^2} \right) \delta_t L \right] \quad (33)$$

The vertical momentum balance over the thermal layer δ_t expresses a balance between the buoyancy forces (the driving forces in natural convection) and the inertia and viscous forces:

$$F'_B \approx F'_I + F'_v \quad (34)$$

where

$$F'_B = -\int_0^L \int_0^{\delta_t} \rho_o g \beta_o (T'_o - T') \, dx' \, dy' \quad (35)$$

$$F'_I = \int_0^L \int_0^{\delta_t} \rho_o (1 + \beta_o (T'_o - T')) \left(u' \frac{\partial v'}{\partial x'} + v' \frac{\partial v'}{\partial y'} \right) dx' \, dy' \quad (36)$$

$$F'_v = \int_0^L \int_0^{\delta_t} \mu_o \left(\frac{\partial^2 v'}{\partial x'^2} + \frac{\partial^2 v'}{\partial y'^2} + \frac{1}{3} \frac{\partial^2 u'}{\partial x' \partial y'} + \frac{1}{3} \frac{\partial^2 v'}{\partial y'^2} \right) dx' \, dy' \quad (37)$$

According to Eqs. (35)–(37) and the scales of the problem, the vertical momentum balance, Eq. (34), can be detailed as follows:

$$[\rho_o g Ga \delta_t L] \approx \left[\left(\rho_o (1 - (\approx Ga)) \frac{V^2}{L} \delta_t L \right) + \approx \left(\mu_o \frac{V}{\delta_t^2} \left(1 + \approx \frac{\delta_t^2}{L^2} \right) \delta_t L \right) \right] \quad (38)$$

Eqs. (33) and (38) establish a system of two equations, in an order of magnitude sense only, with two unknowns: the vertical velocity scale on the thermal layer V and the thermal layer thickness δ_t. Solving this system, the ratio L/δ_t becomes:

$$\frac{L}{\delta_t} \approx \left[\left(\frac{Ra(1 - (\approx Ga))}{Pr^{-1} + \approx 1} \right)^{1/2} + \approx 1 \right]^{1/2} \quad (39)$$

From Eq. (39) it can be observed that, when $Ga > 0$, the ratio L/δ_t and, then, the mean Nusselt number, Eq. (29), is always lower than in the Boussinesq model.

From Eqs. (29) and (39) it follows:

$$Nu = C_1 \left[\left(\frac{Ra(1 - C_2 Ga)}{Pr^{-1} + C_3} \right)^{1/2} + C_4 \right]^{1/2} \quad (40)$$

Eq. (40) can be improved by using the methodology of Churchill and Usagi [40] and therefore placing:

$$Nu^n = 1^n + \left[C_1 \Pi_N^{1/2} \right]^n \quad (41)$$

where Eq. (40) deriving from the present scale analysis, is combined with the limit $Nu = 1$ pertinent to the pure conductive regime.

In Eq. (41):

$$\Pi_N = \left[\left(\frac{Ra(1 - C_2 Ga)}{Pr^{-1} + C_3} \right)^{1/2} + C_4 \right] \quad (42)$$

By means of a general least squares procedure fitting the numerical data of Figs. 2 and 3 and the present predictions of Table 1, the values of the coefficients of Eq. (41) and (42) have been determined as $n = 6$, $C_1 = 0.4828$, $C_2 = 0.011$, $C_3 = 4.992$, $C_4 = -4.588$, yielding the final correlation:

$$Nu = \left[1 + \left(C_1 \Pi_N^{1/2} \right)^6 \right]^{1/6} \quad (43)$$

In Fig. 4 the mean Nusselt number is plotted versus the parameter Π_N. The solid line represents the correlation given by Eq. (43). Symbols represent the present numerical predictions of Figs. 2 and 3 and of Table 1. As can be seen from Fig. 4, Eq. (43) agrees fairly well with the present numerical predictions.

For the same problem, other heat transfer correlations have been proposed by Zhong et al. [16] and Emery and Lee [41]. Both are expressed in the form $Nu = A \cdot Ra_r^m$.

For $780\ (1 + \Theta/T'_r)^{2.7} \leqslant Ra_r \leqslant 10^6$, Zhong et al. [16] proposed:

$$A = (8 + (\alpha_h/\alpha_c)^{0.84})^{-1}, \quad m = 0.322, \quad T'_r \equiv T'_c$$

For $0.01 \leqslant Pr \leqslant 1$ and $10^4 \leqslant Ra_r \leqslant 10^6$, Emery and Lee [41] suggested:

$$A = 0.185 \cdot Pr_r^{0.089}, \quad m = 0.278, \quad T'_r \equiv T'_o$$

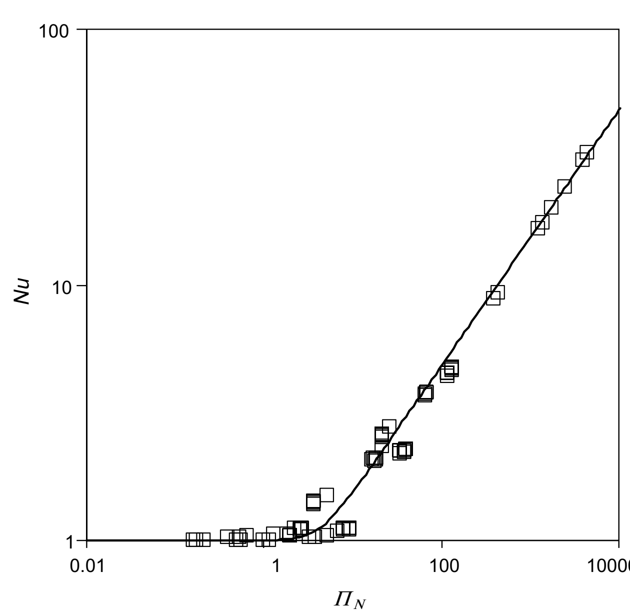

Fig. 4. Variation of the laminar mean Nusselt number with Π_N – (line: correlation; symbol: present predictions).

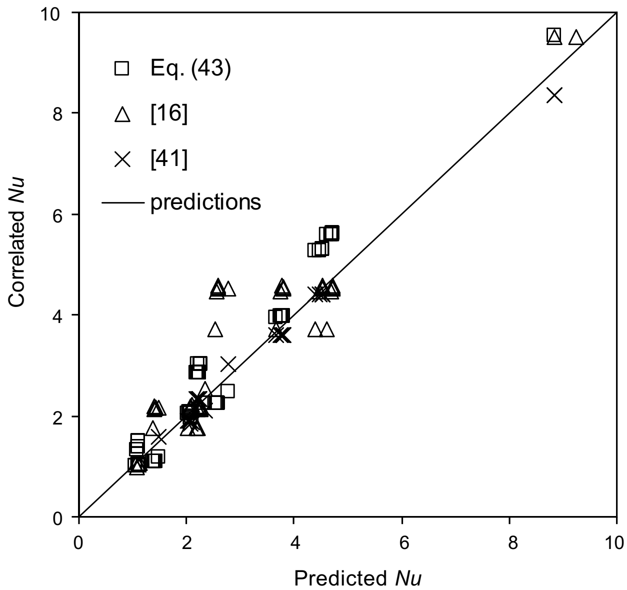

Fig. 5. Comparison of the laminar mean Nusselt number – (line: present predictions; symbols: correlations).

In accordance with these bounds, in Fig. 5 the *Nu* values calculated by Eq. (43) and by the correlations proposed by Zhong et al. [16] and Emery and Lee [41], have been compared with the present *Nu* predictions. The Zhong et al. correlation [16] does not fit with the same accuracy of Eq. (43) the data for the wide Prandtl number range addressed here; the Emery and Lee correlation [41] is valid just for a narrow Rayleigh number range in which, however, it is more accurate than the present one.

5. Concluding remarks

Laminar natural convection in a square cavity heated through the side walls at low Prandtl numbers with large density differences has been investigated numerically and theoretically.

An appropriate dimensionless parameter characterizing the density changes of the working fluid due to the temperature field has been identified as the Gay-Lussac number.

The influence of the Gay-Lussac number on the mean Nusselt number has been derived over all its physical field, $0 \leqslant Ga < 2$, where $Ga = 0$ leads to the Boussinesq assumption. The predictions obtained from the numerical simulation show that the mean Nusselt number decreases as the Gay-Lussac number increases, with highest differences between the corresponding cases under the Boussinesq assumption ranging from 1% to 7%, as the Rayleigh number increases. Furthermore, when $Ga > 0$, the computational effort required to achieve the convergence is $1.5 \div 2$ times that for the cases using the Boussinesq assumption.

The influence of the Prandtl number on the mean Nusselt number has been investigated in the laminar domain. The analysis shows that the mean Nusselt number increases with the Prandtl number and, in particular, its effect is more evident at high Rayleigh numbers.

The influence of the dimensionless parameters *Ra*, *Pr* and *Ga* on the mean Nusselt number has been elucidated by means of a scale analysis: this can be regarded as an extension of that proposed by Arpaci [37] in the case of $Ga > 0$ and a thick thermal layer.

Finally, based on physical arguments, a heat transfer correlation, Eq. (43), has been proposed. This expresses the present numerical predictions with a fairly accurate degree of fidelity, as shown in Figs. 4 and 5.

Acknowledgement

The authors thank Prof. M.W. Collins for the discussions and the revision of the manuscript.

References

[1] S. Ostrach, Natural convection in enclosures, J. Heat Transfer 110 (1988) 1175–1190.
[2] G. de Vahl Davis, Natural convection of air in a square cavity: a bench mark numerical solution, Int. J. Numer. Methods Fluids 3 (1983) 227–248.
[3] P. Le Quéré, Accurate solutions to the square thermally driven cavity at high Rayleigh number, Comput. Fluids 20 (1991) 29–42.
[4] V.A.F. Costa, Laminar natural convection in differentially heated rectangular enclosures with vertical diffusive walls, Int. J. Heat Mass Transfer 45 (2002) 4217–4225.
[5] V.A.F. Costa, M.S.A. Oliveira, A.C.M. Sousa, Control of laminar natural convection in differentially heated square enclosures using solid insert at the corners, Int. J. Heat Mass Transfer 46 (2003) 3529–3537.
[6] M.G. Braunsfurth, A.C. Skeldon, A. Juel, T. Mullin, D.S. Riley, Free convection in liquid gallium, J. Fluid Mech. 342 (1997) 295–314.
[7] W.P. Graebel, The influence of Prandtl number on free convection in a rectangular cavity, Int. J. Heat Mass Transfer 34 (1981) 125–131.
[8] J.L. Lage, A. Bejan, The Ra–Pr domain of laminar convection in an enclosure heated from the side, Numer. Heat Transfer Part A Appl. 19 (1991) 21–41.
[9] S. Saravanan, P. Kandaswamy, Buoyancy convection in low Prandtl number liquids with large temperature variation, Meccanica 37 (2002) 599–608.
[10] R. Derebail, J.N. Koster, Numerical simulation of natural convection of gallium in a narrow gap, Int. J. Heat Mass Transfer 40 (1997) 1169–1180.
[11] I. Di Piazza, M. Ciofalo, Low-Prandtl number natural convection in a volumetrically heated rectangular enclosures. I. Slender cavity, AR = 4, Int. J. Heat Mass Transfer 43 (2000) 3027–3501.
[12] I. Di Piazza, S. Arcidiacono, M. Ciofalo, Low-Prandtl number natural convection in a volumetrically heated rectangular enclosures. II. Square cavity, AR = 1, Int. J. Heat Mass Transfer 44 (2001) 537–550.
[13] S. Arcidiacono, M. Ciofalo, Low-Prandtl number natural convection in a volumetrically heated rectangular enclosures. III. Shallow cavity, AR = 0.25, Int. J. Heat Mass Transfer 44 (2001) 3053–3065.
[14] I. Di Piazza, M. Ciofalo, MHD free convection in a liquid-metal filled cubic enclosure. I. Differential heating, Int. J. Heat Mass Transfer 45 (2002) 1477–1492.
[15] I. Di Piazza, M. Ciofalo, MHD free convection in a liquid-metal filled cubic enclosure. II. Internal heating, Int. J. Heat Mass Transfer 45 (2002) 1493–1511.
[16] Z.Y. Zhong, K.T. Yang, J.R. Lloyd, Variable property effects in laminar natural convection in a square enclosure, J. Heat Transfer 107 (1985) 133–138.
[17] R. Becker, M. Braack, Solution of a stationary benchmark problem for natural convection with large temperature difference, Int. J. Therm. Sci. 41 (2002) 428–439.
[18] J. Vierendeels, B. Merci, E. Dick, A multigrid method for natural convective heat transfer with large temperature differences, J. Comput. Appl. Math. 168 (2004) 509–517.
[19] M. Darbandi, S. Hosseinizadeh, Numerical simulation of thermobuoyant flow with large temperature variation, J. Thermophys. Heat Transfer 20 (2006) 285–296.
[20] H. Paillere, C. Viozat, A. Kumbaro, I. Toumi, Comparison of low Mach number models for natural convection problems, Heat Mass Transfer 36 (2000) 567–573.
[21] ANSYS CFX User Manual, Release 10.0, 2005.
[22] D.C. Wan, B.S.V. Patnaik, G.W. Wei, A new benchmark quality solution for the buoyancy-driven cavity by discrete singular convolution, Numer. Heat Transfer Part B Fundam. 40 (2001) 199–228.
[23] D. Gray, A. Giorgini, The validity of the Boussinesq approximation for liquid and gases, Int. J. Heat Mass Transfer 19 (1976) 545–551.
[24] D.J. Tritton, Physical Fluid Dynamics, second ed., Clarendon Press, Oxford, 1988.
[25] J.P. Catchpole, G. Fulford, Dimensionless groups, Ind. Eng. Chem. 58 (1966) 46–60.
[26] H.W. Hahnemann, Die Umstellung auf das Internationale Einheitensystem in Mechanik und Wärmetechnik, VDI-Verlag, Düsseldorf, 1959.
[27] C. Soong, C. Chyuan, R. Tzong, Thermo-flow structure and epitaxy uniformity in large-scale metal organic chemical vapor deposition reactors with rotating susceptor and inlet flow control, Jpn. J. Appl. Phys. 37 (1998) 5823–5834.
[28] Y. Kim, J. Boo, B. Hong, Y.J. Kim, Effects of showerhead shapes on the flowfields in a RF-PECVD reactor, Surf. Coat. Tech. 193 (2005) 88–93.
[29] H. van Santen, C.R. Kleijn, H.E.A. Van Den Akker, Symmetry breaking in a stagnation-flow CVD reactor, J. Crystal Growth 212 (2000) 311–323.

[30] H. van Santen, C.R. Kleijn, H.E.A. Van Den Akker, On multiple stability of mixed-convection flows in a chemical vapor deposition reactor, Int. J. Heat Mass Transfer 44 (2001) 659–672.
[31] S.P. Vanka, G. Luo, N.G. Glumac, Parametric effects on thin film growth and uniformity in an atmospheric pressure impinging jet CVD reactor, J. Crystal Growth 267 (2004) 22–34.
[32] G. Luo, S.P. Vanka, N.G. Glumac, Fluid flow and transport processes in a large area atmospheric pressure stagnation flow CVD reactor for deposition of thin films, Int. J. Heat Mass Transfer 47 (2004) 4979–4994.
[33] H. Mlaouah, T. Tsuji, Y. Nagano, A study of non-Boussinesq effect on transition of thermally induced flow in a square cavity, Int. J. Heat Fluid Flow 18 (1997) 100–106.
[34] S.A. Suslov, S. Paolucci, Stability of natural convection flow in tall vertical enclosure under non-Boussinesq conditions, Int. J. Heat Mass Transfer 38 (1995) 2143–2157.
[35] S.A. Suslov, S. Paolucci, Stability of non-Boussinesq convection via the complex Ginzburg–Landau model, Fluid Dyn. Res. 35 (2004) 159–203.
[36] A. Bejan, Convection Heat Transfer, Wiley, New York, 1984.
[37] V.S. Arpaci, Buoyant turbulent flow driven by internal energy generation, Int. J. Heat Mass Transfer 38 (1995) 2761–2770.
[38] V.S. Arpaci, A. Agarwal, Scaling laws or turbulent ceiling fires, Combust. Flame 116 (1999) 84–93.
[39] O. Aydin, L. Guessous, Fundamental correlations for laminar and turbulent free convection from an uniformly heated vertical plate, Int. J. Heat Mass Transfer 44 (2001) 4605–4611.
[40] S.W. Churchill, R. Usagi, A general expression for the correlation of rates of transfer and other phenomena, AIChE J. 18 (1972) 1121–1128.
[41] A.F. Emery, J.W. Lee, The effects of property variations on natural convection in a square enclosures, J. Heat Transfer 121 (1999) 57–62.